# EVALUATION OF FORCE-VELOCITY CHARACTERISTICS OF QUADRICEPS MUSCLES BY MEANS OF PEAK TORQUE-ANGULAR VELOCITY RELATIONSHIP DURING KNEE EXTENSION AND FLEXION

by

Abdulaziz Akkılık

B.S., E.E., Istanbul Technical University, 2004

Submitted to the Institute of Biomedical Engineering
in partial fulfillment of the requirements
for the degree of
Master of Science
in
Biomedical Engineering

Boğaziçi University
September 2008

**EVALUATION OF FORCE-VELOCITY CHARACTERISTICS OF QUADRICEPS MUSCLES BY MEANS OF PEAK TORQUE-ANGULAR VELOCITY RELATIONSHIP DURING KNEE EXTENSION AND FLEXION**

**APPROVED BY:**

| | |
|---|---|
| Assistant Prof. Dr. Burak Güçlü<br>(Thesis Advisor) | ……. |
| Prof. Dr. Sabri Altıntaş | ……. |
| Assistant Prof. Dr. Can Yücesoy | ……. |

**DATE OF APPROVAL:** 15 September 2008

# ACKNOWLEDGEMENTS

I would like to express my sincere thanks to my thesis supervisor, Assistant Prof. Dr. Burak Güçlü. He provided me with necessary support, advice, facilities and enthusiasm required to successfully complete this thesis. I would like to thank to Prof. Dr. Ali Haydar Demirel, who provided me with valuable support throughout the experiments. I also would like to thank PhD Physio. Selda Başar for her support and assistance in the experiments.

# ABSTRACT

## EVALUATION OF FORCE-VELOCITY CHARACTERISTICS OF QUADRICEPS MUSCLES BY MEANS OF PEAK TORQUE-ANGULAR VELOCITY RELATIONSHIP DURING KNEE EXTENSION AND FLEXION

In this thesis, an experiment, which shows that there is a relationship between theoretical force-velocity characteristics of a muscle fiber and experimental peak torque-angular velocity characteristics of quadriceps muscle contraction using CYBEX NORM isokinetic dynamometer, is presented. First, the equations of force-velocity relationship for muscle fiber contraction were derived using a special cross-bridge theory. Then, during the experiments, the subject performed knee extension and flexion movements with different angular velocities. In this way, peak torque values at different angular velocities were obtained during eccentric, isometric and concentric contraction of quadriceps muscles. Finally, it was observed that the theoretical curve of force-velocity for muscle fiber contraction could fit the experimental data showing the relationship of peak torque-angular velocity for quadriceps muscles quite well. As a result, although many parameters were not controlled during the experiments, force-velocity curve of the muscles was applicable for different conditions.

**Keywords:** peak torque, angular velocity, force, isometric contraction, concentric contraction, eccentric contraction, isokinetic dynamometer.

# ÖZET

## DİZ UZATMA VE BÜKME SIRASINDAKİ TEPE TORK-AÇISAL HIZ İLİŞKİSİ YARDIMIYLA KUADRİSEPS KASLARININ KUVVET-HIZ KARAKTERİSTİĞİNİN İNCELENMESİ

Bu tezde, bir kas lifinin kasılmasının teorik hız-kuvvet karakteristiği ile bir CYBEX NORM izokinetik dinamometresi yardımı ile elde edilmiş kuadriseps kaslarının kasılmasına ait deneysel tepe tork-açısal hız karakteristiğinin arasındaki ilişkiyi göstermesi amaçlanan bir deney çalışması sunulmaktadır. Öncelikle, bir kas lifinin kasılmasının kuvvet-hız karakteristiğini gösteren denklemler özel bir aktomyozin köprü teorisi yardımıyla elde edildi. Daha sonra, deney bölümünde, farklı açısal hızlarda diz uzatma ve bükme hareketleri gerçekleştirildi. Bu şekilde, farklı açısal hızlarda izometrik, eksentrik ve konsentrik olarak kasılan kuadriseps kaslarına ait tepe tork değerleri ölçüldü. Kuadriseps kaslarının kasılmasının tepe tork-açısal hız ilişkisini gösteren deneysel sonuçların, teorik olarak elde edilen bir kas lifinin kasılmasına ait kuvvet-hız eğrisine çok benzediği görüldü. Sonuç olarak, deneyler sırasında birçok parametre kontrol edilmemesine rağmen, kasılamaya ait kuvvet-hız eğrisi farklı durumlara uygulanabildi.

**Anahtar Sözcükler:** tepe tork, açısal hız, kuvvet, izometrik kasılma, konsentrik kasılma, eksentrik kasılma, izokinetik dinamometre.

# TABLE OF CONTENTS

# LIST OF FIGURES

# LIST OF TABLES

# LIST OF SYMBOLS

| | |
|---|---|
| $P$ | force at the ends of the muscle |
| $V$ | contraction velocity of the muscle |
| $v$ | shortening velocity of the thin filament relative to the thick filament |
| $x$ | the displacement from the equilibrium configuration measured along the thin filament |
| $u(x)$ | population-density function |
| $p(x)$ | force on the thin filament |
| $U$ | total fraction of bridges that are attached |
| $n_0$ | number of cross-bridges in a half sarcomere |
| $A$ | displacement of newly attached bridges |
| $\alpha$ | rate constant for attachment of bridges |
| $N$ | number of sarcomeres that are connected in series to make up the muscle. |
| $\beta$ | rate constant for detachment of bridges |
| $\gamma$ | constant in $p(x)$ |
| $p_1$ | constant in $p(x)$ |
| $B$ | configuration that cross-bridges inevitably break |
| $P^*$ | normalized $P$ to $P_0$ |
| $P_0$ | isometric force |
| $v^*$ | normalized $v$ to $v_{max}$ |
| $\varphi$ | constant in $P^* - v^*$ Equation |
| $A^*$ | constant in $P^* - v^*$ Equation |
| $r^*$ | constant in $P^* - v^*$ Equation |
| T | torque |
| $T_0$ | isometric torque |
| ω | angular velocity |

# LIST OF ABBREVIATIONS

| | |
|---|---|
| SSE | Sum of Squared Error |
| RMSE | Root Mean Squared Error |

# 1. INTRODUCTION

Unlike a simple elastic body, muscle is able to adjust its force to precisely match the load that is experienced during shortening. This remarkable property of muscle is based on the fact that active force continuously adjusts to the speed at which the contractile system moves. Thus, when the load is small, the force produced by the muscle is made correspondingly small by increasing the speed of shortening appropriately. Conversely, when the load is high, the active force is raised to an equivalent level by decreasing the shortening speed sufficiently [1]. The fact that there exists a given relation between load and velocity of shortening in muscle was first demonstrated by Fenn & Marsh [2]. Hill [3] further characterized the force-velocity relation in frog skeletal muscle and pointed out the importance of this parameter for understanding the basic mechanisms of muscle contraction.

The idea that this mechanical behavior of muscle could be explained in terms of the dynamics of the cross bridge population was introduced by A.F. Huxley [4]. More precisely, he proposed a specific cross bridge model that could account for the steady-state force velocity and energetic relationships discovered by A.V. Hill [3]. According to this plausible idea, muscle shortens when interdigitating filaments of fixed length increase their overlap by sliding past one another.

Lacker and Peskin [5] proposed a particular cross bridge theory similar to Huxley's but not quite the same. They explored a new method for testing the cross bridge hypothesis within the context of a class models similar in spirit to A.F. Huxley's 1957 scheme [4]. Detailed properties of the cross bridge were determined uniquely by a systematic mathematical technique that employed data from macroscopic muscle contracting at a constant velocity. The method was tested and applied using data of A.V. Hill [3]. The derived cross bridge properties were used to predict transients obtained when tetanically stimulated muscle was subjected to sudden changes in load.

In this thesis, the particular cross-bridge theory proposed by Lacker and Peskin was basically examined. All force-velocity curves and equations were obtained with the help of

this muscle model during shortening and lengthening of the muscle. The experiment of knee extension and flexion movements was executed to obtain peak torque values of knee extensors -quadriceps muscles- with varying angular velocity of the movement. The experimental results obtained from quadriceps muscles by the help of CYBEX NORM isokinetic dynamometer was compared with the force-velocity curve of the muscle acquired theoretically in the cross-bridge theory. As a result, the experimental data was fitted by the curve defined by the equations found in the cross-bridge theory.

Whereas the experimental data shows the relationship between the angular velocity and the peak torque obtained during quadriceps muscles contraction, in the theory of Lacker and Peskin, the relationship between linear velocity and force of a muscle fiber contraction is discussed. Peak torque was assumed as a measure of strength. As angular velocity and linear velocity values were normalized to their maximum values during the comparison, it was thought that angular velocity and linear velocity would have the same effects on the results. Therefore, this thesis aimed to evaluate force-velocity characteristics of quadriceps muscles by help of peak torque-angular velocity relationship during knee extension and flexion.

# 2. MUSCULAR SYSTEM

## 2.1 Muscle Structure

The function of muscle is to allow movement and to produce body heat. In order to achieve this, muscle tissue must be able to contract and stretch. Contraction occurs via a stimulus from the nervous system. There are three types of muscle tissue; smooth, cardiac and skeletal.

Skeletal muscle by definition is the muscle which is involved in the voluntary movement of the skeleton. It is also called striated muscle as the fibers, which are made up of many cells, are composed of alternating light and dark stripes, or striations. Skeletal muscle can also be contracted without conscious control, for example in sudden involuntary movement [6].

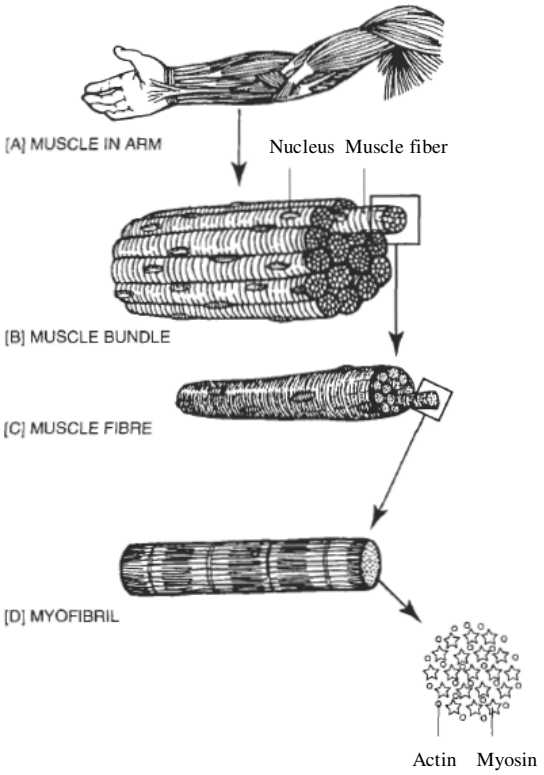


**Figure 2.1** Gross to molecular structure of muscle [6].

Skeletal muscle is composed of cells that have specialized functions. They are called muscle fibers, due to their appearance as a long cylindrical shape plus numerous nuclei. Their lengths range from 0.1 cm to 30 cm with a diameter from 0.01 cm to 0.001 cm. Within these muscle fibers are even smaller fibers called myofibrils. These myofibrils are made up of thick and thin threads called myofilaments. The thick myofilaments are called **myosin** and the thin myofilaments are called **actin**. Myosin and actin filaments, as well as regions where the two overlap, form repeating light and dark bands in each sarcomere. These thick and thin filaments are linked at regular intervals by cross-bridges made from extensions of the myosin molecules Figure 2.1 shows a progression from the gross to the molecular structure of muscle [6].

In each sarcomere, thin myofilaments extend in from each end. Thick myofilaments are found in the middle of the sarcomere and do not extend to the ends. Because of this arrangement, when skeletal muscle is viewed with a microscope, the ends of a sarcomere (where only thin myofilaments are found) appear lighter than the central section (which is dark because of the presence of the thick myofilaments). Thus, a myofibril has alternating light and dark areas because each consists of many sarcomeres lined up end-to-end. This is why skeletal muscle is called striated muscles (i.e., the alternating light and dark areas look like stripes or striations). The light areas are called the **I-bands** and the darker areas the **A-bands**. Near the center of each I-Band is a thin dark line called the **Z-line** (or Z-membrane in Figure 2.2). The Z-line is where adjacent sarcomeres come together and the thin myofilaments of adjacent sarcomeres overlap slightly. Thus, a **sarcomere** can be defined as the area between Z-lines [7].

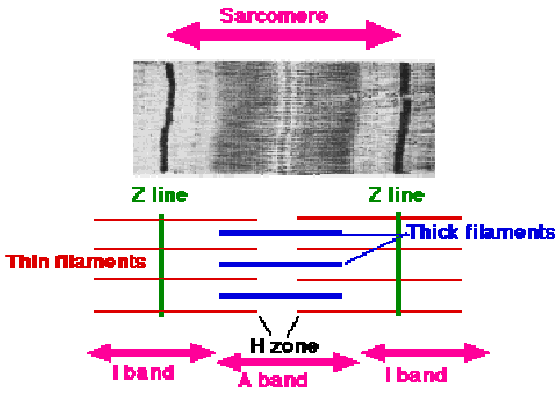


**Figure 2.2** Sarcomere structure [7].

Smooth muscle tissue is so called because it does not have striations and therefore appears smooth under a microscope. It is also called involuntary because it is controlled by the autonomic nervous system. Unlike skeletal muscle, it is not attached to bone. It is found within various systems within the human body, for example the circulatory, the digestive and respiratory. Its main difference from skeletal muscle is that its contraction and relaxation are slower. Also, it has a rhythmic action which makes it ideal for the gastro-intestinal system. The rhythmic action pushes food along the stomach and intestines [6].

Cardiac muscle, as the name implies, is found only in the heart. Under a microscope the fibers have a similar appearance to skeletal muscle. However, the fibers are attached to each other via a specialized junction called an 'intercalated disc'. The main difference between skeletal and cardiac muscle is that cardiac muscle has the ability to contract rhythmically on its own without the need for external stimulation. This of course is of high priority in order that the heart may pump for 24 hour/day. When cardiac muscle is stimulated via a motor end plate, calcium ions influx into the muscle fibers. This results in contraction of the cardiac muscle. The intercalated discs help synchronize the contraction of the fibers. Without this synchronization the heart fibers may contract independently, thus greatly reducing the effectiveness of the muscle in pumping the blood around the body [6].

## 2.2 Mechanism of Muscle Contraction

Control of muscle is achieved via the nervous system. Nerves are attached to muscle via a junction called the motor end plate. Shown in Figure 2.3 is a diagrammatic representation of a motor end plate [6].

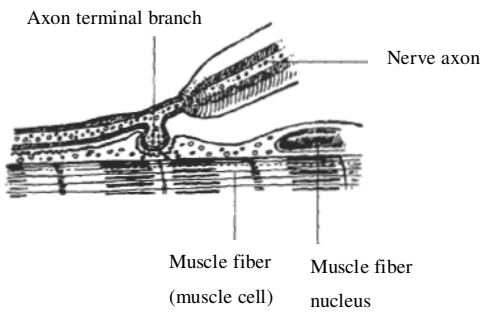


**Figure 2.3** Motor end plate [6].

Muscle has an all or none phenomenon. In order to contract, it has to receive a stimulus of a certain threshold. Below this threshold muscle will not contract; above this threshold muscle will contract but the intensity of contraction will not be greater than that produced by the threshold stimulus.

The mechanism of contraction can be explained with reference to Figure 2.4. A nerve impulse travels down the nerve to the motor end plate. Calcium diffuses into the end of the nerve. This releases a neurotransmitter called acetylcholine, a neural transmitter. Acetylcholine travels across the small gap between the end of the nerve and the muscle membrane. Once the acetylcholine reaches the membrane, the permeability of the muscle to sodium ($Na^+$) and potassium ($K^+$) ions increases. Both ions are positively charged. However, there is a difference between permeability for the two ions. $Na^+$ enters the fiber at a faster rate than the $K^+$ ions leave the fiber. This results in a positive charge inside the fiber. This change in charge initiates the contraction of the muscle fiber [6].

The mechanism of contraction also involves the actin and myosin filaments which, in a relaxed muscle, are held together by small cross bridges. When the muscle is stimulated, the introduction of calcium released from sarcoplasmic reticulum in muscle cells breaks these cross bridges and allows the actin to move using ATP as a fuel. Relaxation of muscle occurs via the opposite mechanism. The calcium breaks free from the actin and myosin and enables the cross bridges to reform. Recently there has been a new theory of muscle contraction. This suggests that the myosin filaments rotate and interact with the actin filaments, similar to a corkscrew action, with contacts via the cross bridges. The rotation causes the contraction of the muscle [6].

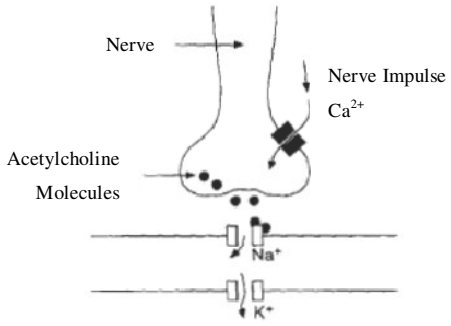


**Figure 2.4** Mechanism of muscle contraction [6].

# 3. MUSCLE MECHANICS

## 3.1 Cross-Bridge Dynamics

Researchers from 1930 to 1960 sought to understand the mechanism of muscle contraction. The "contracting filament hypothesis" proposed that the filaments themselves contract. Electron microscope observations, however, did not support this hypothesis. Neither the thick nor thin bands changed in length when the muscle contracted. Only the degree of overlap between thick and thin filaments changed. Huxley alternatively proposed the **Sliding Filament Model**, suggesting muscle contraction results as the cross bridges linking the actin and myosin molecules pull the filaments over one another (Figure 3.1) [7].

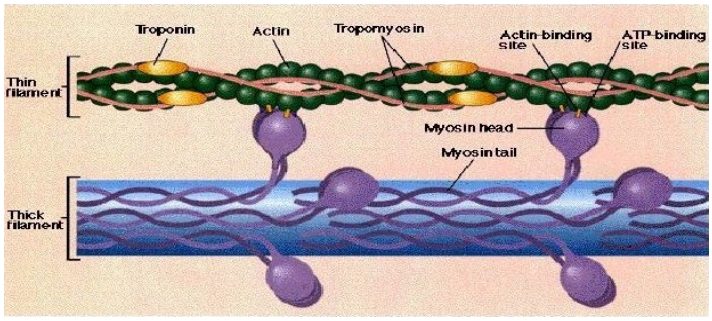


**Figure 3.1** The structures of thin and thick filaments [7].

According to Huxley's idea, the cross-bridges, arm like projections from the thick filaments connect and disconnect with the thin filaments in response to the composition of their chemical environment. Immediately after such a connection is established, a chemical reaction occurs that puts the cross-bridge into a strained configuration. The cross-bridge then pulls the thin filament toward the center of the sarcomere. A second chemical reaction leads to breakage of the cross-bridge connection to the thin filament. This is referred to as the cross-bridge cycle [8].

The smooth contraction of the sarcomere is brought about by the combined activity of the entire cross-bridge population. The events of attachment and detachment occur essentially at random and independently in different cross-bridges. The chemical environment of the sarcomere governs the mean attachment and detachment rates. On the

other hand, the motions of the attached cross-bridges are coordinated since these motions are determined by the sliding velocity of the filaments. The sliding velocity is the same for all of the cross-bridges in a sarcomere. As the sliding of the filament carries the cross-bridge away from its initial configuration, the strain of that configuration is relieved, and the force on the thin filament is reduced. At higher velocities of shortening, this happens faster. Thus, the muscle develops smaller forces at higher velocities of shortening. This effect explains, qualitatively at least, the form of the force-velocity curve determined below [9].

## 3.2 The Force-Velocity Curve

An important property of muscle is the relationship between the force $P$ which it generates and the velocity $V$ of its shortening. Observations of muscle under tension reveal a relationship between force and shortening speed like that shown in Figure 3.2 [8].

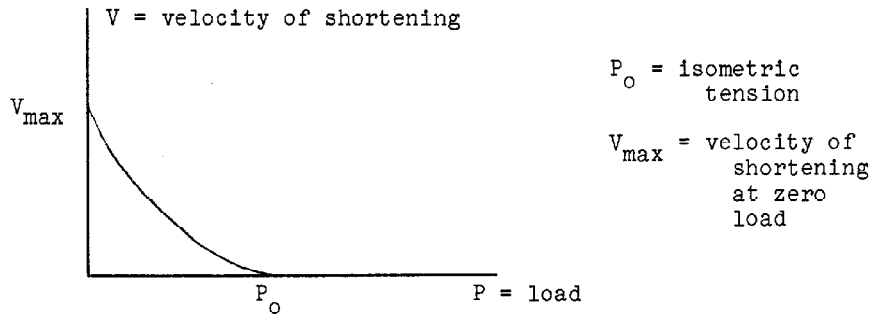


**Figure 3.2** Relationship between force and shortening velocity [9].

The force-velocity curve characterizes a muscle in a constant contractile state. Such a state can be achieved in an isolated muscle by rapid, repetitive electrical stimulation. In life, a constant contractile state is achieved by sending a steady stream of nerve impulses to signal the muscle to contract. A muscle in a constant contractile state (and within a certain range of lengths) shortens at a rate that is determined by the load (or force) at the ends of the muscle. It is this relationship that is depicted in Figure 3.2.

Two important points on the force-velocity curve are its intercepts with the coordinate axes: When $P = 0$, the muscle shortens at its maximum velocity, $V_{max}$. As the load is increased, the velocity of shortening gets smaller, until the **isometric force**, $P_0$, is reached, at which the muscle cannot shorten ($V = 0$).

A.V. Hill was first to notice that the experimental force-velocity curves are closely fitted by an equation of the form

$$V = b\,(P_0 - P)\,/\,(P + a) \tag{3.1}$$

where $P_0$ is the isometric force, and $a$ and $b$ are constants that can be determined from the experimental data. $P_0$ is the force at which contraction does not occur at the same time [8]. From the equation above, $V_{max}$ can be determined by setting $P = 0$ and solving for $V$. The result is

$$V_{max} = bP_0a. \tag{3.2}$$

While Hill's Equation (3.1) supports the experimental force-velocity curves closely for shortening, the speed of lengthening is much smaller than would be expected from an extrapolation of Hill's Equation to the negative velocity region. If the force applied to the muscle rises above a threshold, the muscle increases length very rapidly. In other words when the force is greater than 1.8 $P_0$, the muscle gives. This means that the muscle behaves as if it loses its ability to resist stretching (Figure 3.3).

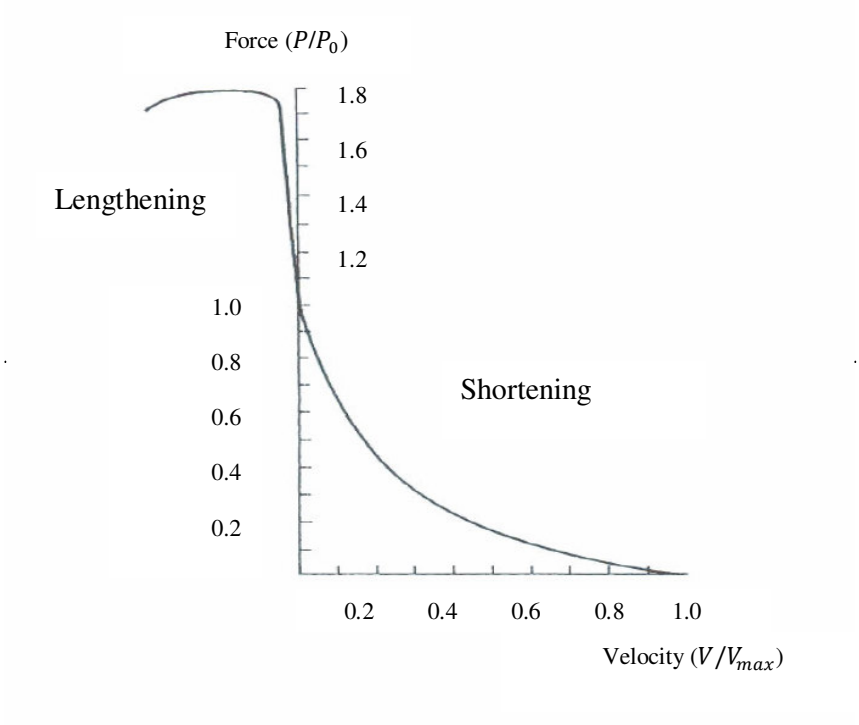


**Figure 3.3** Force-velocity curves for both shortening and lengthening [10].

In general, it is observed that if a muscle is shortening rapidly it cannot generate as much force as when it is stationary, and even a greater force is required to stretch an active

muscle. Figure 3.4 tries to make this clear. The maximum weights can be lifted change during bench pressing in different situations. The maximum weight can be lifted off the chest rapidly is quite low. The maximum weight lifted slowly is somewhat higher, and the maximum weight maintained the height of is higher still. An even higher weight will force the trainer to lower it slowly. This relates exactly to graph in Figure 3.3. A muscle applying force without shortening is known as an **isometric** contraction. A muscle applying force and shortening is a **concentric** contraction. A muscle applying force but being extended anyway is performing an **eccentric** contraction [11].

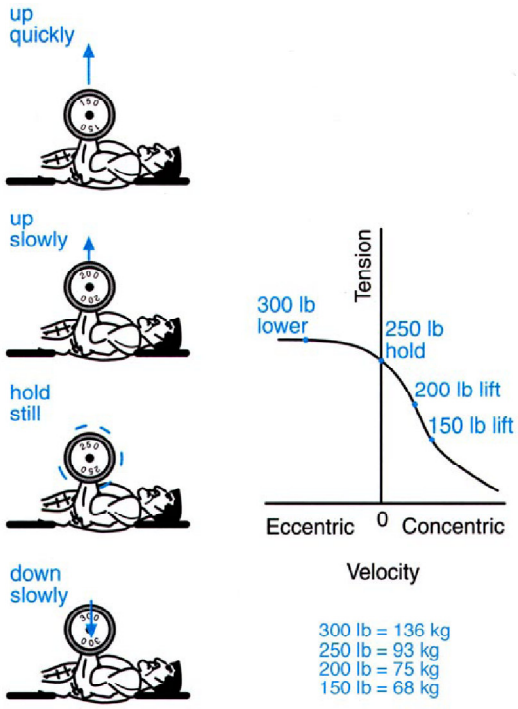


**Figure 3.4** An example for force-velocity relationship of the muscle [11].

Concentric muscle activity is what it is typically thought about muscles doing. It is not cared much about isometric activity but it is used all the time to maintain posture. Eccentric muscle activity is also common and is often used at the ends of activities to slow down movements and is obviously used in situations when energy is being lost such as walking down stairs or landing from a jump. Figure 3.5 shows some examples [11].

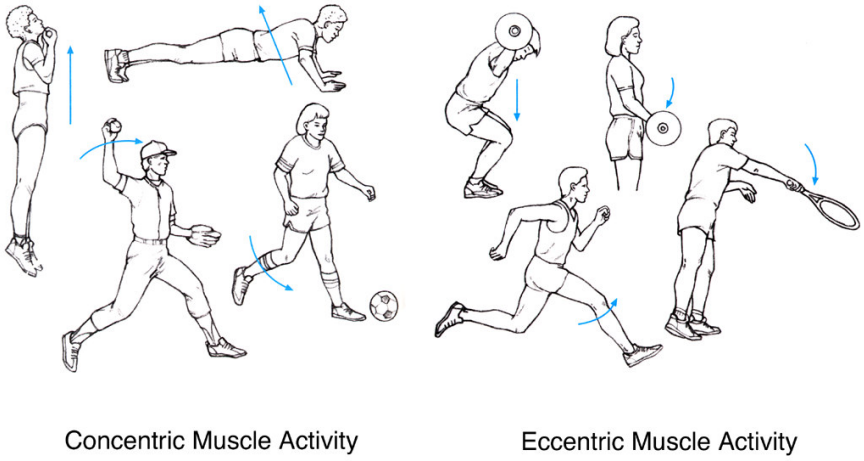


**Figure 3.5** Examples of concentric and eccentric muscle activity [11].

# 4. MUSCLE MODEL FORMULATION

## 4.1 Cross-Bridge Theory of Lacker and Peskin

According to this theory [8], an attached cross-bridge has an equilibrium configuration in which it exerts no force on the thin filament and $x$ denotes the displacement from this equilibrium configuration measured along the thin filament (Figure 4.1).

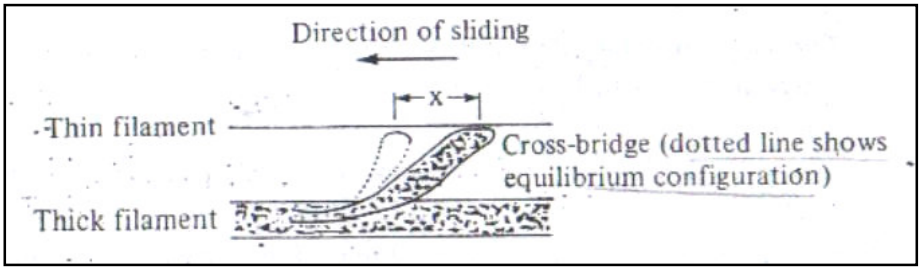


**Figure 4.1** Cross-bridge dynamics [8].

$p(x)$ is the force on the thin filament when the displacement of the cross-bridge is equal to $x$. Obviously, $p(0) = 0$, since $x = 0$ is the equilibrium configuration of an attached cross-bridge, and that $p(x)$ is an increasing function of $x$. And, $n_0$ is the number of cross-bridges in a half sarcomere. These entire cross bridges are effectively in parallel (their forces add), and all of the half sarcomeres are effectively in series (their lengths add). Accordingly, the force on the ends of the muscle if all cross-bridges are attached and have displacement $x$ would be $n_0\, p(x)$.

In general, the different cross-bridges have different values of $x$ and so, cross-bridge population is described by the population-density function $u(x)$ defined by

$$\int_{x2}^{x1} u(x)dx. \tag{4.1}$$

The integral of $u(x)$ between the borders $x_1$ and $x_2$ gives the fraction of bridges with displacement $x$. The total fraction of bridges that are attached is given by

$$U = \int_{-\infty}^{\infty} u(x)dx \; < 1 \tag{4.2}$$

The force on the ends of the muscle, $P$, is also given by an integral over the cross-bridge population:

$$P = n_0 \int_{-\infty}^{\infty} p(x)\, u(x) dx \tag{4.3}$$

The cross-bridge cycle consists of attachment, sliding and detachment. The key assumption is that cross-bridge population is in a steady state. So, these three process rates must balance in this steady state. Meanwhile, it is assumed that all cross bridges form their attachments in a certain configuration $x = A > 0$.

Attachment rate is proportional to the number of bridges that are available for attachment at any given time. So, this rate can be written as $\alpha\, n_0\, (1 - U)$, where the constant $\alpha$ is called rate constant for attachment and has units of time$^{-1}$.

Sliding rate is the shortening velocity of the thin filament relative to the thick filament and satisfies the equation $dx/dt = -v$ and also, $v = V/2N$ where $V$ is the macroscopic velocity of shortening for the whole muscle and $N$ is the number of sarcomeres that are connected in series to make up the muscle.

Finally, the rate of detachment can be written as $\beta\, n_0\, U$. This rate is proportional to the number of attached bridge and $\beta$ is called the rate constant for bridge detachment. If all attention is restricted to those bridges that have $x$ in some particular interval, $(x_1, x_2)$, then the number of such bridges (per half sarcomere) is

$$n_0 \int_{x2}^{x1} u(x) dx \tag{4.4}$$

and the rate at which these bridges break is

$$\beta\, n_0 \int_{x2}^{x1} u(x) dx. \tag{4.5}$$

To find $u(x)$, an interval of $x, x_0 < x < A$, is selected. Since cross-bridges are formed at $x = A$ and are moved by sliding in the direction of decreasing $x$, it is important that $u(x) = 0$ for $x > A$. Within this interval, three rates must balance (Figure 4.2). This gives the equation

$$\alpha\, n_0\, (1 - U) = \beta\, n_0 \int_{x_0}^{A} u(x)\, dx + v\, n_0\, u(x_0)\,. \tag{4.6}$$

$\alpha\, n_0\, (1 - U)$ is attachment rate of the new bridges, $\beta\, n_0 \int_{x_0}^{A} u(x)\, dx$ is breaking rate of the attached cross-bridges in the interval of $x_0 < x < A$ . $v\, n_0\, u(x_0)$ is sliding rate at $x = x_0$.

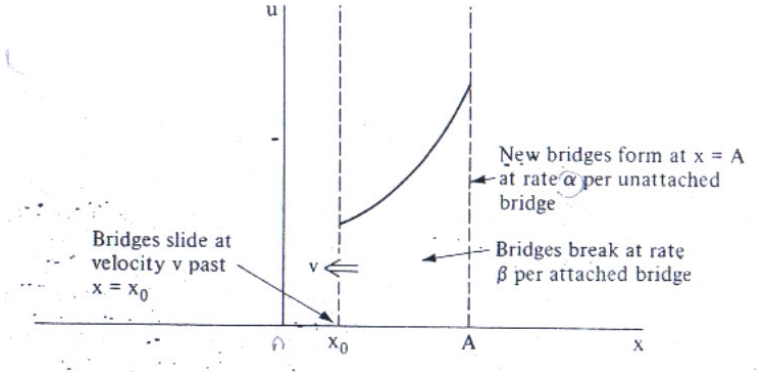


**Figure 4.2** Balance state in the interval $x_0 < x < A$ [8].

This integral equation (4.6) for $u$ can be used to derive both a differential equation that holds for $x < A$, and a boundary condition that holds at $x = A$. To get the differential equation, Equation (4.6) is differentiated with respect to $x_0$. The result is

$$0 = -\beta\, u(x_0) + v\, (du/\, dx)(x_0). \tag{4.7}$$

This equation can be written more simply as

$$v\, (du/\, dx) = \beta\, u. \tag{4.8}$$

Solutions of this equation have the form

$$u(x) = u(A)\, exp(\beta(x - A)/v). \tag{4.9}$$

The constant $u(A)$ in Equation (4.9) is not yet determined, however. Besides, Equation (4.9) is valid only when $x < A$. For $x > A, u(x) = 0$.

An equation is derived for $u(A)$, using Equation (4.6) and setting $x_0 = A$. The result below is acquired.

$$\alpha\, (1 - U) = v\, u(A) \tag{4.10}$$

This equation asserts that new bridges are carried away from $x = A$ as fast as they are formed.

Unfortunately, Equation (4.10) does not quite determine $u(A)$ since $U$ is still unknown. Integrating Equation (4.9) from $-\infty$ to $A$, it is found that

$$U = \int_{-\infty}^{A} u(x)\, dx = v\, u(A)\, /\, \beta. \tag{4.11}$$

This gives another relationship between $U$ and $u(A)$, so Equations (4.10) and (4.11) can be solved as a pair of linear equations in these two unknowns. The result is

$$U = \alpha / (\alpha + \beta) \tag{4.12}$$

$$u(A) = \alpha \beta / (v(\alpha + \beta)) \tag{4.13}$$

so that for $x < A$

$$u(x) = \alpha \beta \, exp(\beta(x - A)/v)/[v(\alpha + \beta)] \tag{4.14}$$

and $u(x) = 0$ if $x > A$. This result is plotted in Figure 4.3 using the values in Table 4.1 for two different sliding velocities $v$.

**Table 4.1**
Symbols used in the cross bridges theory and their values [14].

| Symbol | Value | Unit | Meaning of symbol |
|---|---|---|---|
| $\alpha$ | 14 | 1/s | rate constant for attachment of bridges |
| $\beta$ | 126 | 1/s | rate constant for detachment of bridges |
| $p_1$ | 4 | pN | constant in $p(x)$ |
| $n_0$ | 10000 | - | number of cross-bridges in a half sarcomere |
| $\gamma$ | 0.322 | 1/nm | constant in $p(x)$ |
| $A$ | 5 | nm | displacement of newly attached bridges |
| $v$ | - | nm/s | velocity of the thin filament relative to the thick filament |
| $P$ | - | pN | force on the ends of the muscle |

But, for Figure 4.3, $A$ is assumed as 15 nm. For low $v$, selected as 300 nm/s, the bridges are clustered near $x = A$, whereas for high $v$, selected as 900 nm/s, they are more spread out in the direction of negative $x$.

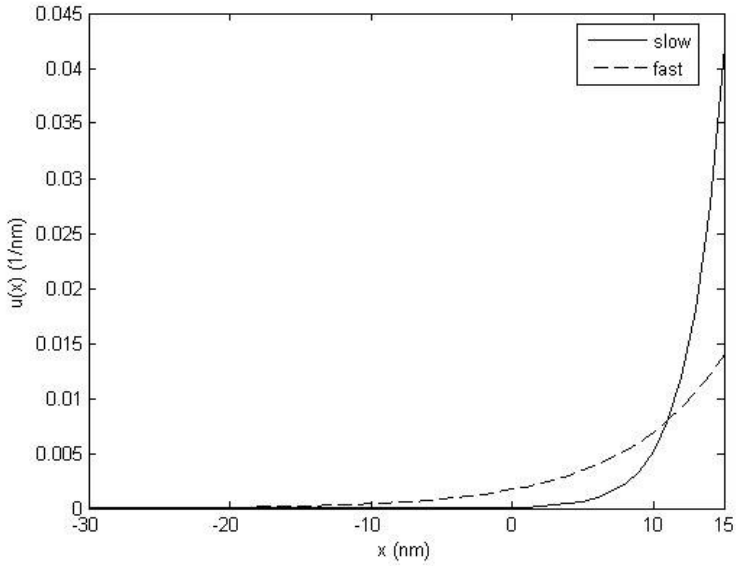


**Figure 4.3** Population density function, $u(x)$ for shortening.

Having determined the behavior of the cross-bridge population, the equation for the force-velocity curve is calculated. From Equation (4.3), it is obtained that

$$P = [\alpha\beta/(v(\alpha+\beta))] \int_{-\infty}^{A} n_0 p(x) exp(\beta(x-A)/v)\, dx. \quad (4.15)$$

To proceed further, $p(x)$, the force exerted by a single cross-bridge in configuration $x$, is needed. If $p(x)$ is assumed as below (Figure 4.3),

$$p(x) = p_1(exp(\gamma x) - 1) \quad (4.16)$$

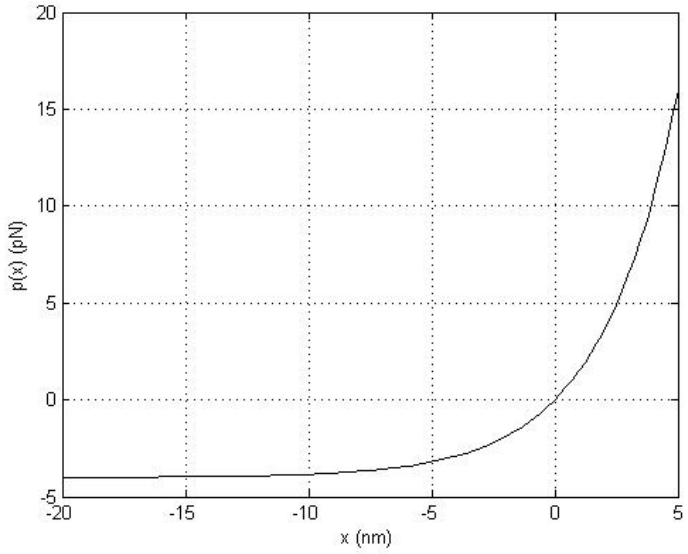


**Figure 4.4** The force exerted by a single cross-bridge, $p(x)$. In the graph, the values in Table 4.1 are used. $p(x) = 0$ for $x > A$ and $p(x) \rightarrow -p_1$ as $x \rightarrow -\infty$.

and substituted in Equation (4.15), evaluating the integral,

$$P = [\alpha\, n_0\, p_1/(\alpha+\beta)][((e^{\gamma A} - 1) - (\gamma v/\beta))/(1 + (\gamma v/\beta))] \quad (4.17)$$

the formula for the force-velocity curve is obtained. Solving for $\gamma v/\beta$,

$$\gamma v/\beta = [(\alpha\, n_0\, p_1/(\alpha+\beta))(e^{\gamma A} - 1) - P]/[P + \alpha\, n_0\, p_1/(\alpha+\beta)] \quad (4.18)$$

is acquired. This has the same form as the empirical force-velocity curve in Equation (3.1). Since the velocity $V$ at the ends of the muscle is related to $v$ according to $V = 2Nv$, as indicated before

$$V = b(P_0 - P)/(P + a) \quad (4.19)$$

where the constants $P_0$, $b$, and $a$ are now given by the formulae

$$P_0 = (\alpha\, n_0\, p_1/(\alpha+\beta))(e^{\gamma A} - 1) \quad (4.20)$$

$$b = 2N\beta/\gamma \quad (4.21)$$

$$a = \alpha\, n_0\, p_1/(\alpha+\beta) \quad (4.22)$$

Since $V_{max} = bP_0/a$,

$$V_{max} = (2N\,\beta/\gamma)\,(e^{\gamma A} - 1) \tag{4.23}$$

is obtained substituting the variables.

As a result, Peskin and Lacker have thus derived the empirical force-velocity curve from a particular model of cross-bridge dynamics, and determined the relationship between the microscopic properties of the model cross-bridges and macroscopic constants of the muscle [8]. The formula for the isometric force, $P_0$, can be explained by the observation that all of the attached cross-bridges have the configuration $x = A$ and $v = 0$. Thus, the force exerted by each of these bridges is $p(A) = p_1(exp(\gamma A) - 1)$. Since the number of attached bridges is $\alpha\, n_0/(\alpha + \beta)$, $P_0$, is given by Equation (4.20).

The maximum velocity of shortening is determined by setting $P = 0$. This means that the negative forces exerted by the cross-bridges with $x < 0$ balance the positive forces exerted by the cross-bridges with $x > 0$. The velocity at which this occurs is independent of overall size of the cross-bridge population. So, $V_{max}$ is independent of $\alpha\, n_0$.

It is interesting to contrast the behavior of $P_0$ and $V_{max}$ with respect to the parameter $\beta$, which is the rate of detachment of cross-bridges. Increasing $\beta$ decreases $P_0$ by decreasing the number of attached bridges. When $\beta$ increases, $V_{max}$ increases, however, because rapid detachment prevents most bridges from sliding into negative values of $x$ where they would oppose shortening. A muscle with high $\beta$ is fast but weak; a muscle with low $\beta$ is slow but strong [8].

All the equations till here belong to Lacker and Peskin. After that point, I performed all following derivations in the next parts by the help of the Cross-Bridge Theory of Lacker and Peskin. During this process, some assumptions were changed.

### 4.1.1 Linear Force-Velocity Curve

Lacker and Peskin assumed that the force exerted by a single cross bridge in configuration $x$,

$$p(x) = p_1(exp(\gamma x) - 1). \tag{4.24}$$

If it is assumed that $p(x) = kx$ and $p(x)$ is substituted in (4.15), evaluating the integral

$$P = n_0 \alpha\, k\, (A - v/\beta)/\,(\alpha + \beta) \tag{4.25}$$

is obtained. Solving for $V = 2Nv$, the equation

$$V = A2N\beta - [P(\alpha + \beta)2N\beta / n_0\alpha k] \quad (4.26)$$

is acquired. It is seen that the formula for the force-velocity curve while $p(x) = kx$ leads to a linear force-velocity curve. Also, the equations

$$V_{max} = A\,\beta\,2N \quad (4.27)$$

$$P_0 = n_0\,\alpha\,k\,A/(\alpha + \beta) \quad (4.28)$$

are acquired. In fact, noticing that $p(x) = kx$ is a limiting case of an exponential spring; the same results are obtained. That is,

$$p_1(e^{\gamma x} - 1) = p_1\gamma x(e^{\gamma x} - 1)/\gamma x \rightarrow kx \quad (4.29)$$

as $\gamma \rightarrow 0, p_1 \rightarrow \infty$, but with $p_1\gamma = k$. Having this observation, if the corresponding limit in Equation (4.19) through Equation (4.23) is taken, the same results above are obtained.

## 4.2 Cross Bridge Theory While Stretching

When a force greater than the isometric force, $P_0$, is applied to a muscle, the muscle stretches at a velocity depending on the applied force. To prove this event mathematically, making the same assumptions that were made above for shortening, some changes should be made for stretching.

Stretch is treated as a negative velocity of shortening ($v < 0$). Cross-bridges still form at $x = A$, but now they are carried into the region $x > A$ by sliding process. So, $u = 0$ for $x < A$, and the equation that replaces Equation (4.6) is

$$\propto (1 - U) = \beta \int_A^{x_0} u(x)dx - v\,u(x_0). \quad (4.30)$$

This integral equation (4.30) for $u$ can be used to derive both a differential equation that holds for $x > A$, and a boundary condition that holds at $x = A$. To get the differential equation, Equation (4.30) is differentiated with respect to $x_0$. The result is

$$0 = \beta\,u(x_0) - v\,(du/dx)(x_0) \quad (4.31)$$

This equation can be written more simply as

$$v\,(du/dx) = \beta\,u \quad (4.32)$$

Solutions of this equation have the form

$$u(x) = u(A)\,exp(\beta(x - A)/v). \quad (4.33)$$

The constant $u(A)$ in Equation (4.33) is not yet determined, however. Besides, Equation (4.33) is valid only when $x > A$. For $x < A, u(x) = 0$.

An equation is derived for $u(A)$, going back to Equation (4.30) and setting $x_0 = A$. The result is

$$\alpha\,(1 - U) = -v\;u(A) \tag{4.34}$$

which asserts that new bridges are carried away from $x = A$ as fast as they are formed.

Unfortunately, Equation (4.34) does not quite determine $u(A)$ since $U$ is still unknown. Integrating Equation (4.33) from $A$ to $\infty$, it is acquired that

$$U = -v\,u(A)\,/\,\beta \tag{4.35}$$

This gives another relationship between $U$ and $u(A)$, so Equations (4.34) and (4.35) can be solved as a pair of linear equations in these two unknowns. The result is

$$U = \alpha\,/\,(\alpha + \beta) \tag{4.36}$$

$$u(A) = -\alpha\,\beta\,/\,(v(\alpha + \beta)) \tag{4.37}$$

so that for $x > A$

$$u(x) = -\alpha\,\beta\,exp(\beta(x - A)/v)/[v(\alpha + \beta)] \tag{4.38}$$

and $u(x) = 0$ if $x < A$. This result is plotted in Figure 4.5 according to the values in the Table 4.1, for two different sliding velocities $v$. For low $v$, the bridges are clustered near $x = A$, whereas for high $v$ they are more spread out in the direction of positive $x$.

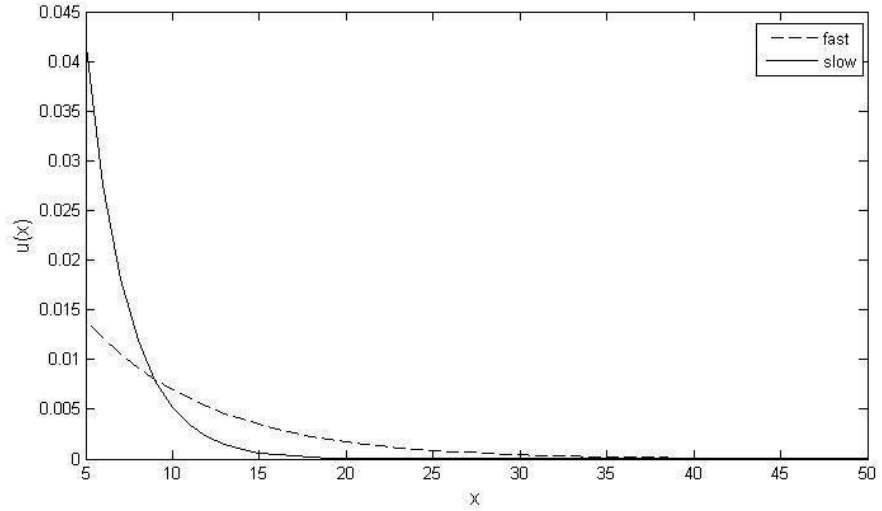


**Figure 4.5** Population density function, $u(x)$, during stretching

Having determined the behavior of the cross-bridge population, the equation for the force-velocity curve is calculated. From the Equation (4.3), the equation below is obtained integrating from $A$ to $\infty$.

$$P = \left[-\alpha\,\beta\,p_1\,n_0/(v(\alpha + \beta)\right]\;\int_A^{\infty}(\exp\,(\gamma x) - 1)\left(\exp\left(\frac{\beta(x-A)}{v}\right)\right)dx. \tag{4.39}$$

After evaluating the integral, the equation for force-velocity curve in the interval $-\beta/\gamma < v < 0$ is found

$$P = [\alpha\, n_0\, p_1/(\alpha+\beta)][((e^{\gamma A}-1)-(\gamma v/\beta))/(1+(\gamma v/\beta))]. \quad (4.40)$$

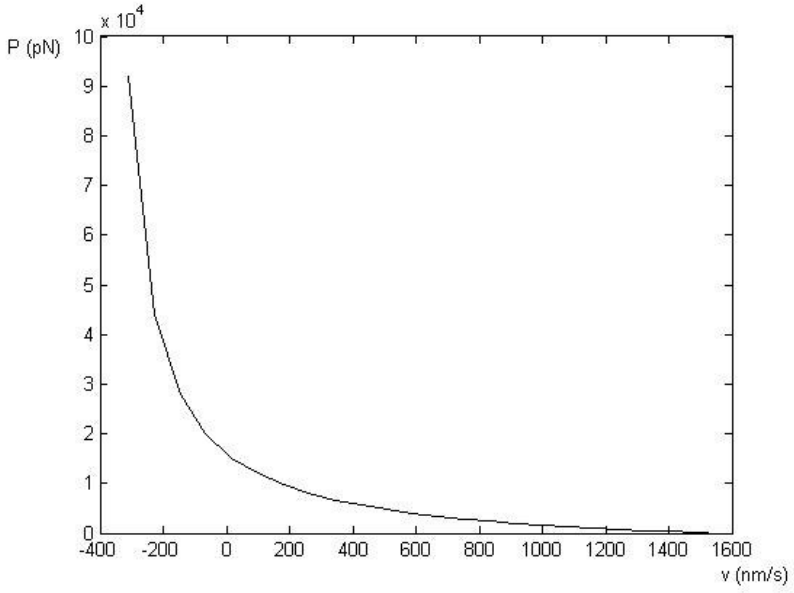


**Figure 4.6** Force-velocity curve for positive and negative velocities of shortening

## 4.3 Cross Bridge Theory during Muscle Yielding

As seen above (Figure 4.6), the part of the force velocity curve for stretch, negative velocity of shortening ($v < 0$), predicts infinite force at a finite velocity, $v = -\beta/\gamma$. This is very unrealistic. In fact, muscles yield when the applied force is greater than 1.8 $P_0$. That is, there is a maximum force that the muscle can sustain.

To explain this kind of behavior, the cross-bridge model should be modified by assuming that bridges inevitably break if they reach a configuration $x = B$, where $B > A$. This has no effect on the force-velocity curve for shortening, but it does influence the force-velocity curve of lengthening, since all of the integrals now extend over the integral $(A, B)$ instead of $(A, \infty)$.

The Equation (4.30), written for cross bridge population in a steady state, does not change. Therefore, the equations for $u(x)$, from Equation (4.33) to Equation (4.34) are valid for yielding. $U$, the total fraction of bridges that are attached, is defined in Equation

(4.2). As $u(x) = 0$ for $x < A$ and $x > B$, the new equation is $U = \int_A^B u(x)dx$. Evaluating the integral, it is found that

$$U = u(A)\left(\frac{v}{\beta}\right)\left(\exp\left(\frac{\beta(B-A)}{v}\right) - 1\right). \tag{4.41}$$

Using Equations (4.41) and (4.34), the equation below is acquired:

$$u(A) = \alpha\beta/[v(\alpha(\exp(\beta(B-A)/v) - 1) - \beta)\,]. \tag{4.42}$$

This Equation (4.42) is put in Equation (4.33), the equation for $u(x)$. Having determined the behavior of the cross-bridge population, the equation for the force- velocity curve is acquired integrating the Equation (4.3) from $A$ to $B$

$$P = n_0\, u(A) p_1 \int_A^B (\exp(\gamma x) - 1)\exp\left(\frac{\beta(x-A)}{v}\right) dx. \tag{4.43}$$

After evaluating the integral,

$$P^* = \frac{\left(1+\frac{1}{r^*}\right)\left[\frac{\exp(A^*)\left(\exp\left(\varphi+\frac{\varphi}{(\exp(A^*)-1)v^*}\right)-1\right)}{(\exp(A^*)-1)v^*+1} - \exp\left(\frac{\varphi}{(\exp(A^*)-1)v^*}\right)+1\right]}{\left[(\exp(A^*)-1)\left(\exp\left(\frac{\varphi}{(\exp(A^*)-1)v^*}\right)-1-\frac{1}{r^*}\right)\right]} \tag{4.44}$$

is acquired as a formula for the force-velocity curve of lengthening after the last change on the model. This result is expressed in terms of the dimensionless variables $P^* = P/P_0$, $v^* = v/v_{max} = (\gamma v)/[\beta(exp(A^*) - 1)]$ and in terms of dimensionless parameters $r^* = \alpha/\beta$, $A^* = \gamma A$, and $\varphi = \gamma(B - A)$.

Here, $P_0$ is isometric force, defined in Equation (4.20) and $v_{max}$ is the maximum velocity of contraction at end of a sarcomere, obtained dividing Equation (4.23) by $2N$. As Equation (4.23) is the maximum velocity of contraction at the ends of whole muscle, it is divided by $2N$ to get $v_{max}$. Besides, as it is known that $V = 2Nv$, it is accepted that $v/v_{max} = V/V_{max}$.

To sketch the behavior of the force velocity curve for shortening and lengthening together, the force-velocity equation for shortening, Equation (4.17) is rewritten in terms of $P^*$, $v^*$, and $A^*$. Then the equation below is obtained:

$$P^* = \left(\frac{\exp(A^*)}{v^*(\exp(A^*)-1)+1} - 1\right)/(\exp(A^*) - 1). \tag{4.45}$$

In Figure 4.7, the force-velocity curves defined above are plotted while $r^* = A^* = \varphi = 1$ for both shortening and lengthening. As seen in the figure, the change on the model for lengthening prevents the unrealistic situation in Figure 4.6. Here, it is obvious

that there is a maximum force that the muscle can sustain. According to the Figure 4.7, this value is about 1.6 $P_0$. This value can change if different values of $r^*$, $A^*$and $\varphi$ are selected. Here, it is important to show that there is maximum force that the muscle can sustain.

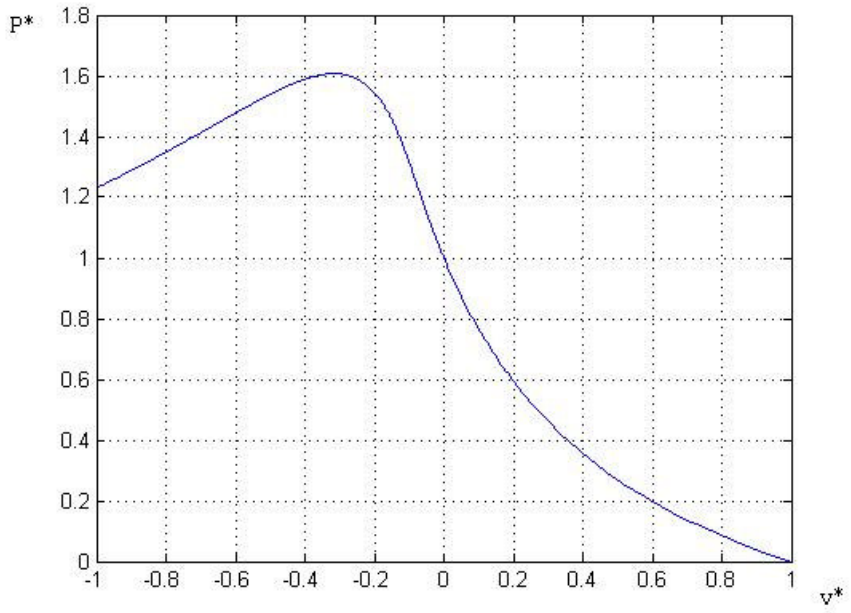


**Figure 4.7** Force-velocity curve ($P^*$-$v^*$)for both shortening and lengthening.

The cross-bridge model was thus modified by assuming that bridges inevitably break if they reach a configuration $x = B$, where $B > A$. Consequently, a finite maximum force is obtained in Figure 4.7. In other words, as $u(x)$, population density function is defined between $x = A$ and $x = B$, a maximum force that a muscle can sustain is acquired. But, in Figure 4.6, force goes to $\infty$ at a finite velocity of lengthening as $u(x)$ goes from $x = A$ to $x = \infty$.

# 5. EXPERIMENTAL METHODS

## 5.1 Subjects

One male volunteer was used as a subject in the experiments. The age of the subject was 26 and the weight of the subject was 61 kg. The experiments did not pose any harm and they adhered to the US National Institutes of Health ethical guidelines for testing human subjects. The subject did not have any muscular or articular problems that could interfere with the experiments. The right leg of the subject was used to measure the desired parameters during the experiments.

## 5.2 Materials

A CYBEX NORM isokinetic dynamometer was used during the experiments. Contralateral limb stabilizer, knee/hip adapter, knee/hip pad and lumber cushion were used as additional parts of isokinetic dynamometer. This dynamometer could execute three types of contraction; isokinetic, isotonic and isometric contractions. In the experiments, isokinetic eccentric, isokinetic concentric and isometric contraction types were executed by the help of isokinetic dynamometer.

**Figure 5.1** CYBEX NORM Isokinetic Dynamometer

The movements of knee extension and flexion were done by the subject while sitting at the chair during the experiments. The isokinetic dynamometer could adjust the angular velocity of the movement and show the torque forming during the movement. In this way, the contraction velocity and force of the quadriceps muscles (Figure 5.2) of the subject were measured in terms of angular velocity and peak torque.

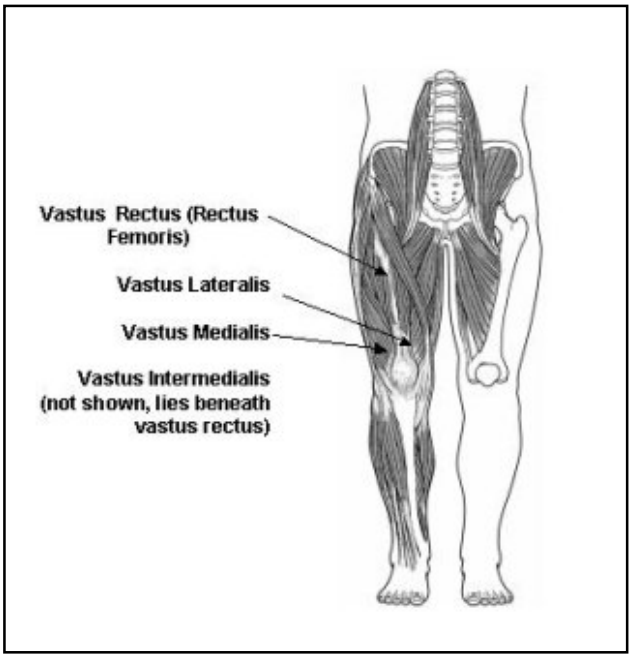


**Figure 5.2** The Quadriceps Muscles, also called knee extensors **[**15**].**

It is known that torque is caused by force applied about an axis of rotation. It is an instantaneous measurement, taken by the CYBEX NORM isokinetic dynamometer at every half-degree in the range of motion. The equation for torque is:

$$\text{Torque} = \text{Force} \times \text{Distance} \tag{5.1}$$

where distance indicates the perpendicular distance from the input of force to the center of rotation. Because the CYBEX NORM isokinetic dynamometer measures torque directly at the center of rotation, the force and distance components are not measured (Figure 5.3). For this experiment, the force resulting in all torques was the force occurring at the quadriceps muscles. Consequently, it was assumed that the torque measured by the system was proportional to the force occurring at the quadriceps muscles of the subject. Besides, the amount of torque that can be produced is related to musculotendinous tension levels, joint contact forces and, in some cases, joint translation forces. These points were neglected for the experimental measurements [13].

During the experiments, the peak torque values were observed as peak torque is indicative of maximum muscular tension capability [13]. These torques were produced by the tension of the right quadriceps muscles of the subject on the rotation axis, in other words at the right knee of the subject.


**Figure 5.3** Extension and flexion patterns with isokinetic dynamometer [13]

## 5.3 Procedure

The subject performed knee extension and flexion sessions five times a day. The experiment lasted eight weeks taking measurements at only one day for each week. All the measurements were conducted by the same experimenter to avoid inter-tester variability. Subject was positioned on an adjustable chair and secured to the equipment with straps across the trunk, hip and thigh. The alignment between the dynamometer rotational axis and the knee joint rotation axis was checked at the beginning of each trial. Range of motion was set at $10^0$- $90^0$ ($0^0$ corresponding to knee fully extended). Before each test the gravity compensation procedure was performed according to the manufacturer's instructions. The subject was instructed to push as hard as possible against a shin pad secured to the distal tibia. The shin pad was attached about 5 cm proximal to the lateral malleoulus by using a strap. The subject was asked to position his arms across the chest with each hand clasping the opposite shoulder during the maximal effort trials. On-line visual feedback of the instantaneous dynamometer torque was provided to the subject on a computer screen.

For each knee extension-flexion movement, subject was first asked to make a trial repetition of the movement. Each movement for different angular velocities was repeated two times. The higher peak torque was selected between the results for analyses. For both concentric and eccentric repetitions, subject was instructed to push / resist as hard and as fast as possible and to complete the full range of motion. For each contraction mode and velocity, subject recovered passively for 30 seconds between the measurements. The CYBEX NORM software consistently indicated visually and verbally the duration of the rest phases. Three types of contraction were respectively executed by the subject: isometric, concentric and eccentric contractions.

During isometric contraction; calf of the subject was hold at different degrees from $0^0$ to $90^0$ by the help of the dynamometer. The subject pushed his calf against the shin pad as hard as possible during 5 seconds. At each degree, peak torque values were measured and among these values, maximum peak torque was accepted as the peak torque during isometric contraction. In this way, the length of the muscle did not change and the peak torque of the movement, in other words, the force formed by the quadriceps muscles, was found.

Second, the concentric contraction was executed. During this type of contraction, the subject moved his calf from $90^0$ to $0^0$ with different angular velocities supported by the isokinetic dynamometer. These angular velocities were respectively 50, 100, 150, 200, 300, 350, 400 and 450 degree/second. Higher angular velocities were not supported by the isokinetic dynamometer, and the subject could not move his calf with higher angular velocities. The quadriceps muscles of the subject shortened during this movement. The angular velocity of the movement was accepted as shortening velocity of the quadriceps muscles. At each angular velocity, the peak torque forming as a result of the motion was measured by the isokinetic dynamometer and was shown on the screen of the computer.

Finally, the quadriceps muscles of the subject contracted eccentrically. At this time, the movement was at the opposite direction according to concentric contraction. The calf of the subject was moved from $0^0$ to $90^0$ with different angular velocities by the isokinetic dynamometer. The subject tried to stop the movement with his all power at each time. As a result of the subject's resistance against to the movement, torque occurred and the peak torque during the movement was measured by the system. The angular velocity was

between 0 and 300 degree/second and it was raised 10 degree/second at each contraction. The maximum angular velocity supported by the system was 300 degree/second.

# 6. RESULTS

## 6.1 Results of the Experiment

Isometric contraction was executed at different degrees at the range of motion between $0^0$ and $90^0$. At each angle, peak torque values were noted (Table 6.1). Among these values, the peak torque value was accepted as 214 Nm. This value was called as $T_0$, the maximum torque that can be produced by the quadriceps muscles when they isometrically contract. At this table, force-length characteristics of the muscle are seen. It can be thought that while the calf is at the position of $45^0$, the length of the quadriceps muscles is about resting length, $l_0$, where the maximum number of cross-bridges forms.

**Table 6.1**
The peak torque values for different calf positions at the range of motion.

| Position | Peak torque |
|---|---|
| $15^0$ | 103 Nm |
| $30^0$ | 150 Nm |
| $45^0$ | 214 Nm ($T_0$) |
| $60^0$ | 195 Nm |
| $75^0$ | 187 Nm |
| $90^0$ | 173 Nm |

Secondly, the peak torque values were listed for each different angular velocity during the concentric contraction. It is seen that peak torque decreases as the angular velocity of the movement increases (Table 6.2).

For angular velocities higher than 350 degree/second, peak torque does not change significantly. As a reason, it was assumed that subject cannot push his calf with angular velocities higher than 350 degree/second. Consequently, maximum angular velocity, $\omega_{max}$, was accepted as 350 degree/second. Besides, the peak torque and angular velocity values were respectively normalized to $T_0$, peak torque during isometric contraction, and $\omega_{max}$.

**Table 6.2**
The peak torque values for different angular velocities during concentric contraction

| No | Peak Torque T (Nm) | Angular speed ω (°/sec) | $T/T_0$ | $\omega/\omega_{max}$ |
|---|---|---|---|---|
| 1 | 214 | 0 (isometric) | 1.000 | 0.000 |
| 2 | 183 | 50 | 0.855 | 0.143 |
| 3 | 148 | 100 | 0.692 | 0.286 |
| 4 | 107 | 150 | 0.500 | 0.429 |
| 5 | 78 | 200 | 0.364 | 0.571 |
| 6 | 49 | 250 | 0.229 | 0.714 |
| 7 | 47 | 300 | 0.220 | 0.857 |
| 8 | 23 | 350 (max. speed) | 0.107 | 1.000 |
| 9 | 20 | 400 | | |
| 10 | 22 | 450 | | |

Finally, the peak torque values were evaluated during the eccentric contraction (Table 6.3). All peak torque values and angular velocities were normalized to $T_0$ and $\omega_{max}$ respectively.

The angular velocities were shown with a minus sign, showing that the quadriceps muscles extend and the movement is at the opposite direction according to concentric contraction. It is seen that all peak torque values except the values at the angular velocities of 290 and 300 degree/second are above the peak torque value of isometric contraction, $T_0$. Maximum and minimum peak torque values for eccentric contraction are respectively 1.243 $T_0$ and 0.958 $T_0$. The peak torque reaches the highest value at -0.429 $\omega_{max}$. In general, the peak torque firstly increases until the angular velocity reaches about -0.3 $\omega_{max}$. After that point, the peak torque remains about 1.2 $T_0$. When the angular velocity approaches to -0.8 $\omega_{max}$, the peak torque starts to decrease. For the velocities higher than -0.8 $\omega_{max}$, the value of peak torque remains under isometric contraction level. The object could not resist against these angular velocities higher than -0.8 $\omega_{max}$.

**Table 6.3**
The peak torque values for different angular velocities during eccentric contraction

| No | Peak Torque T (Nm) | Angular speed ω (°/sec) | $T/T_0$ | $\omega/\omega_{max}$ |
|---|---|---|---|---|
| 1 | 205 | -300 | 0.958 | -0.857 |
| 2 | 205 | -290 | 0.958 | -0.829 |
| 3 | 226 | -280 | 1.056 | -0.800 |
| 4 | 245 | -270 | 1.145 | -0.771 |
| 5 | 252 | -260 | 1.178 | -0.743 |
| 6 | 257 | -250 | 1.201 | -0.714 |
| 7 | 255 | -240 | 1.192 | -0.686 |
| 8 | 259 | -230 | 1.210 | -0.657 |
| 9 | 258 | -220 | 1.206 | -0.629 |
| 10 | 252 | -210 | 1.178 | -0.600 |
| 11 | 257 | -200 | 1.201 | -0.571 |
| 12 | 250 | -190 | 1.168 | -0.543 |
| 13 | 255 | -180 | 1.192 | -0.514 |
| 14 | 251 | -170 | 1.173 | -0.486 |
| 15 | 260 | -160 | 1.215 | -0.457 |
| 16 | 266 | -150 | 1.243 | -0.429 |
| 17 | 255 | -140 | 1.192 | -0.400 |
| 18 | 260 | -130 | 1.215 | -0.371 |
| 19 | 264 | -120 | 1.234 | -0.343 |
| 20 | 255 | -110 | 1.192 | -0.314 |
| 21 | 261 | -100 | 1.220 | -0.286 |
| 22 | 252 | -90 | 1.178 | -0.257 |
| 23 | 250 | -80 | 1.168 | -0.229 |
| 24 | 257 | -70 | 1.201 | -0.200 |
| 25 | 246 | -60 | 1.150 | -0.171 |
| 26 | 232 | -50 | 1.084 | -0.143 |
| 27 | 225 | -40 | 1.051 | -0.114 |
| 28 | 230 | -30 | 1.075 | -0.086 |
| 29 | 220 | -20 | 1.028 | -0.057 |
| 30 | 222 | -10 | 1.037 | -0.029 |

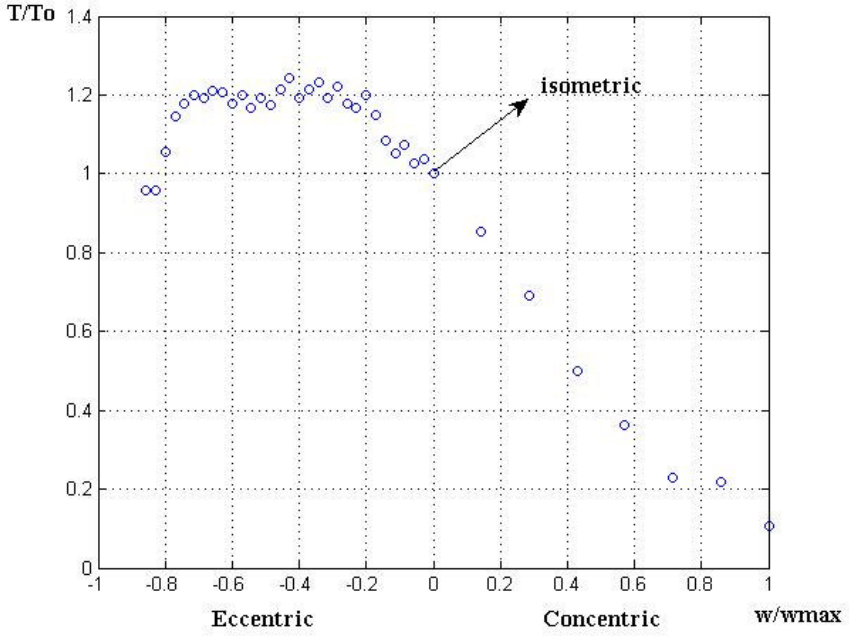


**Figure 6.1** The graph of normalized peak torque-angular velocity for quadriceps muscles

The graph above shows the relationship between normalized angular velocity and peak torque of the quadriceps muscles during the experiments (Figure 6.1). According to this graph, all peak torque values during concentric contraction are smaller than peak torque during isometric contraction. For eccentric contraction, peak torque values -except two values- are higher than these of both isometric and concentric contraction.

## 6.2 Force-Velocity Curve & Experimental Data Comparison

After acquiring the graph of the relationship between angular velocity and torque for muscle contraction as an experimental data (Figure 6.1), the result was compared with the theoretical force-velocity curves and equations for muscle contraction in the cross-bridge theory suggested by Lacker and Peskin [5]. There were two different equations of the relationship between velocity and force for muscle contraction. One of them was for isometric and concentric contraction, the other was for eccentric contraction.

First, the experimental data for isometric and concentric contraction was compared with theoretic force-velocity curve. Equation (4.45), as seen below,

$$P^* = \left(\frac{\exp(A^*)}{v^*(\exp(A^*)-1)+1} - 1\right) / (\exp(A^*) - 1) \qquad (6.1)$$

shows the relationship between force and velocity for isometric and concentric contraction. Using Curve Fitting Tool interface in MATLAB, experimental data was fitted by a curve defined by Equation (4.45) (Figure 6.2).

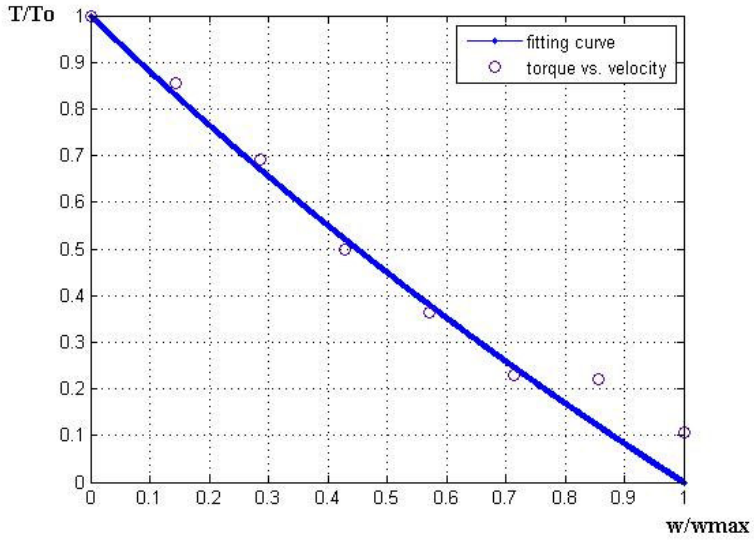


**Figure 6.2** The experimental data and fitting curve for isometric and concentric contraction

As a result of fitting, the parameter $A^*$ was found as 0.2027 (Table 6.4). This parameter was used in the equation for eccentric contraction with the same value, as the same muscles were used for all contraction types. The variables $P^*$ and $v^*$ in the equation were accepted as $T/T_0$ and $\omega/\omega_{max}$ respectively.

**Table 6.4**
Results for the curve fitting the experimental data during isometric and concentric contraction.

| Coefficients (with 95% confidence bounds): $A^*$= 0.2027 (-0.06416, 0.4696) | |
|---|---|
| **Goodness of Fit** | |
| SSE (sum of squared error) | 0.02069 |
| R-square | 0.9719 |
| Adjusted R-square | 0.9719 |
| RMSE (Root Mean Squared Error) | 0.05437 |

Secondly, the experimental data for eccentric contraction was fitted by a curve defined by Equation (4.44), as seen below (Figure 6.3).

$$P^* = \frac{\left(1+\frac{1}{r^*}\right)\left[\frac{\exp(A^*)\left(\exp\left(\varphi+\frac{\varphi}{(\exp(A^*)-1)v^*}\right)-1\right)}{(\exp(A^*)-1)v^*+1}-\exp\left(\frac{\varphi}{(\exp(A^*)-1)v^*}\right)+1\right]}{\left[(\exp(A^*)-1)\left(\exp\left(\frac{\varphi}{(\exp(A^*)-1)v^*}\right)-1-\frac{1}{r^*}\right)\right]} \quad (6.2)$$

This equation gives the relationship between force and velocity during eccentric contraction. Taking the value of $A^*$ as same as in the first fitting, the variables $r^*$ and $\varphi$ were found as 14.92 and 0.1041 respectively from the fitting results (Table 6.5).

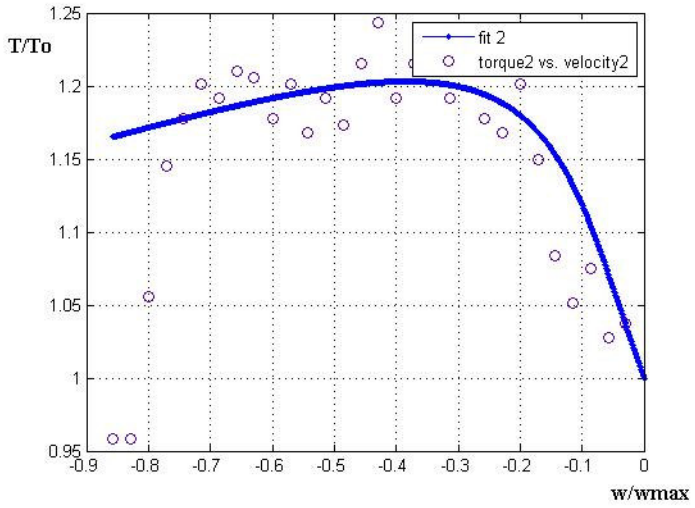


**Figure 6.3** The experimental data and fitting curve for eccentric contraction

For both fittings, curves were acquired with Nonlinear Least Squares Method using Curve Fitting Tool in MATLAB. As SSE and RMSE get closer to 0 and R-square and Adjusted R-square get closer to 1, the fitting becomes better. These values in Table 6.4 and 6.5 were acquired selecting the best goodness of fit among all curves obtained by changing fit options in Curve Fitting Tool of MATLAB.

**Table 6.5**
Results for the curve fitting the experimental data during eccentric contraction.

| | |
|---|---|
| Coefficients (with 95% confidence bounds): | $A^*$= 0.2027 (fixed at bound) |
| | $r^*$= 14.92 (-2.558, 32.4) |
| | $\varphi$= 0.1041 (0.08055, 0.1277) |
| **Goodness of Fit** | |
| SSE (sum of squared error) | 0.04255 |
| R-square | 0.769 |
| Adjusted R-square | 0.7607 |
| RMSE (Root Mean Squared Error) | 0.03898 |

# 7. DISCUSSION

As mentioned before, the cross-bridge theory suggested by Lacker and Peskin shows the relationship between linear contraction velocity and the force generated on the ends of the muscle during contraction [8]. In the thesis, knee extension and flexion movements were executed with different angular velocities during experiments. In this way, quadriceps muscles were shortened and stretched with different linear velocities. Beside, measuring the peak torque for each different velocity during the contraction, the maximum force generated on the ends of quadriceps muscles was obtained. Consequently, $P^*$ and $v^*$ in Equations (4.44) and (4.45) were respectively accepted as $T/T_o$ and $\omega/\omega_{max}$ measured during the experiments. At the results of experiments, it was found that $P^* - v^*$ characteristics of the muscle fiber contraction and $T/T_o$ - $\omega/\omega_{max}$ characteristics of quadriceps muscles contraction have similar properties. Such a good fitting between two different characteristics was very amazing. Because, many researches show that even if we control joint motion by fixing the joint for isometric contraction or rotating it at a constant speed for concentric and eccentric contractions, muscle fiber behavior cannot be derived easily [24, 25, 26, 27].

First, force-velocity characteristics of the muscle contraction were obtained for a muscle fiber, while peak torque-angular velocity relationship was acquired for whole quadriceps muscles. The force resulting in the peak torque was generated by whole quadriceps muscles and also biceps femoris muscles during the experiments. Musculotendinous tension levels, joint contact forces and, in some cases, joint translation forces also affect the torque measured by the experimental system. Lieb and Perry [18] reported that the Vastus Lateralis, one of the four quadriceps muscles, makes the greatest contribution to the force produced by the quadriceps muscles from $90^0$ flexion to $0^0$ extension but that the degree of contribution by each muscle to knee extension varies with the knee joint angle. These effects on peak torque were neglected during experiment. But, the normalized peak torque, $T/T_o$, and angular velocity, $\omega/\omega_{max}$, values were used to plot the graphs. Therefore, it was thought that this normalization operation probably reduced the effects of the neglected factors on the results.

Second, torque is multiplication of force and the perpendicular distance from the input of force to the center of rotation. Therefore, it does not mean that the peak torque always shows the point where the maximum force is generated by the muscle when the perpendicular distance, in other words moment arm, changes [11]. Previous studies showed that the joint angle at which the peak torque was observed was found to shift distally in the range of motion as the angular velocity increases [16, 19, 20]. Moreover, moment arm changes as a function of knee joint angle and angular velocity [21]. In this way, peak torque values are measured and compared at different muscle lengths [17]. Because of that, some researchers have claimed that instead of peak torque values, torque should be evaluated at constant muscle length over different angular velocities. They have assumed that changes in the joint angle are equivalent to changes in the muscle length and to changes in the length of muscle fibers. They have proposed angle specific torque for knee extension for studying force-velocity characteristics of human muscles [22, 23]. Neglecting these approaches, peak torque-angular velocity relationship was used to evaluate force-velocity characteristics of quadriceps muscles.

In spite of all assumptions and neglected factors, force-velocity characteristics of quadriceps muscles were evaluated by means of peak torque-angular velocity relationship during knee extension and flexion. Although some researchers have questioned this method [22, 23], recent studies concluded that the evaluation of force-velocity characteristics of knee extensor muscles from isokinetic testing should be done by means of peak torque rather than the angle specific torque like in the present study [24, 25]. Reeves et al. [26] demonstrated that a constant fiber length cannot be assumed from the same joint angle during concentric contractions of different angular velocities. Many studies showed that the angle specific condition would not be equivalent to identical muscle fiber length, but rather to unequal muscle fiber length [24, 25]. Even, Kawakami et al. [24] suggested that muscle fibers were at the same length at different peak-torque angles and velocities stating that the change in muscle-tendon unit length (muscle length) by peak-torque angle shift was almost exactly matched by series elastic component elongation. They obtained that result during isokinetic and isometric knee extension. The experimental peak torque-angular velocity relationship obtained from isokinetic and isometric knee extension of the present study is in line with previous studies [24, 25].

According to the results, it was seen that there is a similarity between the theoretical $P^* - v^*$ characteristics of the muscle contraction and the experimental $T/T_o - \omega/\omega_{max}$ characteristics of muscle contraction. The experimental data could be fitted well in the form of Equations (4.44) and (4.45) which were obtained for the $P^* - v^*$ characteristics of the muscle contraction in cross-bridge theory (Figure 7.1). For concentric and isometric contraction, when the experimental data is fitted by the curve defined by Equation (4.45), the dimensionless parameter $A^* = \gamma A$, was found as 0.2027. This parameter was used in Equation (4.44) with the same value, as eccentric contraction was executed by the same muscles. When the experimental data for eccentric contraction was fitted by the curve defined by Equation (4.44), the dimensionless parameters; $r^* = \alpha/\beta$ and $\varphi = \gamma(B - A)$ were found as 14.92 and 0.1041 respectively.

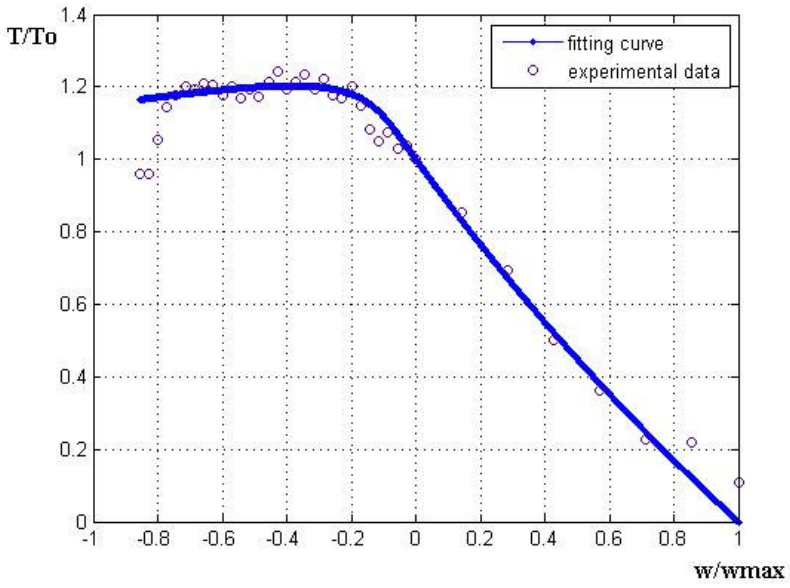


**Figure 7.1** Experimental data and fitting curve defined by force velocity equation in cross bridge theory

These results shows that $\alpha/\beta \cong 15$ and $B \cong 1.5\ A$. In other words, rate constant for attachment of the cross bridges, $\alpha$, is 15 times bigger than rate constant for detachment of the cross bridges, $\beta$ for the quadriceps muscles in the experiments. Recalling that all cross-bridges are assumed to form their attachments in a certain configuration $x = A$, the results show that cross-bridges inevitably break when they reach the configuration $x = 1.5\ A$.

It is seen that there is a significant difference between experimental data and theoretical fitting curve after the angular velocity of eccentric contraction reaches -0.8 $\omega_{max}$. As mentioned before, the subject tried to stop the movement during eccentric contraction. For slow angular velocities, the subject was accomplished about completing the full range of motion. But, for higher angular velocities than -0.8 $\omega_{max}$, the subject could not complete the full range of motion resisting as hard as possible. In the experiment, the movement was affected not only by muscles but also by joints and tendons. These factors limited the maximum lengthening velocity of the quadriceps muscles. Therefore, peak torque values started to decrease after reaching the angular velocity -0.8 $\omega_{max}$. In fact, some experimental results show that force level of the muscles remains about the peak level even if they are lengthened with a velocity higher than 2 $V_{max}$ [12]. But, in these experiments, isolated muscles were used and there was no factor limiting the contraction of the muscles. As the fitting curve at Figure 7.1 shows the behavior of these isolated muscles, peak torque remains about 1.2 $T_0$ for angular velocities higher than -0.8 $\omega_{max}$. Besides, it is seen that maximum torque during eccentric contraction is about 1.2 $T_o$, although some research shows that strength of the muscles increases up to 1.6 $P_0$ [12]. Eccentric actions in situ produce force far smaller than its physiological limit predicted by the experiments with isolated fibers.

Although the experimental data could be fitted well in the form of Equations (4.44) and (4.45) which were obtained for the $P^* - v^*$ characteristics of the muscle fiber contraction in cross-bridge theory, the value of $r^* = \alpha/\beta$ is not in line with physiological data for the eccentric contractions [14]. This problem confronts the concept that force-velocity characteristics can be evaluated by means of peak torque-angular velocity relationship during eccentric contraction, in this study, for knee flexion. Reeves and Narici [26] demonstrated that muscle fascicles contracted quasi-isometrically, independent of angular velocity during eccentric muscle actions. They measured the isokinetic torque at a constant joint angle at different angular velocities. These results show that for the eccentric contraction, it is better to use angle specific torque instead of peak torque to evaluate the force-velocity characteristics of knee extensor muscles.

This thesis can be improved by studying on angle specific torque-angular velocity relationship during knee extension and flexion. The experimental data is fitted by theoretical force-velocity curve. The new values of variables in force-velocity equation are

compared with those of in this study. Beside, maximum shortening velocity for the quadriceps muscles should be higher to obtain more accurate results. In this study, maximum angular velocity, 350 degree/second, represents only 50% of the estimated maximal shortening velocity for knee extensors [23].

In conclusion, it was very surprising that the experimental data showing peak torque-angular velocity relationship of quadriceps muscles during knee extension and flexion could be fitted by the force-velocity curve of a muscle fiber contraction quite well. The present study suggests that peak torque values should be analyzed during isometric and concentric contractions and angle specific torque should be used during eccentric contractions to evaluate the force-velocity characteristics of the quadriceps muscles.

# APPENDIX A. MATLAB CODES

## A.1 MATLAB Code for Population-Density Function $u(x)$

```
alpha=14;          % /s  probability per unit time for attachment
beta=126;          % /s  probability per unit time for detachment
A=5;               % nm displacement of newly attached crossbridge
v=900;             % nm/s shortening velocity
%  v is negative for lengthening
x=[-50:A];         % nm the interval of  x
%  this interval replaces with  [A:50] during lengthening
u=[alpha*beta/(v*(alpha+beta))]*exp(beta*(x-A)/v);   % the equation for u(x)
%  this equation replaces with [-alpha*beta/(v*(alpha+beta))]*exp(beta*(x-A)/v) during
%  lengthing
plot(x,u);
```

## A.2 MATLAB Code for Population-Density Function $p(x)$

```
GAMMA=0.322    %  /nm   constant used in the fuction p(x)
p1=4           %  /pN   constant used in the fuction p(x)
A=5            %   nm   displacement of newly attached crossbridge
x1=linspace(-20,A);
p_1=zeros(1,length(x1));
for i=1:length(x1)
   p_1(i)=p1*(exp(GAMMA*x1(i))-1);     % the equation for p(x)
end
plot (v1,p_1);
```

## A.3 MATLAB Code for $P^* - v^*$ Curve during Shortening

```
A=1;                          % dimensionless parameter in P* − v* equation
p_1=linspace(0,1,10000);      % the interval of P*
 v1=zeros(1,length(p_1));
 for i=1:length(p_1)
    v1(i)=((exp(A)/((p_1(i)*(exp(A)-1))+1))-1)/(exp(A)-1);   % P* − v* equation
end
plot(v1,p_1);
```

## A.4 MATLAB Code for $P^* - v^*$ Curve during Lengthening

```
v2=linspace(-1,0,10000);      % the interval of v*
p_2=zeros(1,length(v2));
w=1;                          % dimensionless parameter in P* − v* equation
r=1;                          % dimensionless parameter in P* − v* equation
A=1;                          % dimensionless parameter in P* − v* equation
for i=1:length(v2)
p_2(i)=((1+1/r)/(exp(A)-1))*(1/(exp(w/(v2(i)*(exp(A)-1)))-1-
        1/r))*(((exp(A)*(exp(w+(w/(v2(i)*(exp(A)-1))))-1))/(v2(i)*(exp(A)-1)+1))-
        exp(w/(v2(i)*(exp(A)-1)))+1);  % P* − v* equation
  end
plot(v2,p_2)
```

# REFERENCES


1. Edman, K. A. P., "Double-hyperbolic force-velocity relation in frog muscle fibres," *J Physiol,* Vol. 404, pp. 301-321, 1988.

2. Fenn, W. O., and B. S. Marsh, "Muscular force at different speeds of shortening," *Journal of Physiology,* Vol. 85, pp. 277-297, 1935.

3. Hill, A. V., "The heat of shortening and the dynamic const ants of muscle," *Proceeding of the Royal Society B,* Vol. 126, pp. 138-195, 1938.

4. Huxley, A. F. "Muscle structure and theories of contraction," *Progress in Biophysics,* Vol. 7, pp. 255-318, 1957.

5. Lacker, H. M., and C. S. Peskin, "A mathematical method for the unique determination of cross-bridge properties from steady state mechanical and energetic experiments on macroscopic muscle," *Vol. 16 of Lectures on Mathematics in the Life Sciences*, pp. 121-153, American Mathematical Society, Providence, RI, 1986.

6. Jennings, D., A. Flint, B. C. H. Turton, and L. D. M. Nokes, *Introduction to Medical Electronics Applications*, Edward Arnold, London, 1995.

7. Huxley, A. F., *Reflections on Muscle* (The Sherrington Lectures XIV). Princeton University Press, Princeton, NJ, 1980.

8. Hoppensteadt, F. C., and C. S. Peskin, *Mathematics in Medicine and the Life Sciences,* New York: Springer-Verlag, 3rd ed., 1996.

9. Katz, B., "The relation between force and speed in muscular contraction," *Journal of Physiology,* Vol. 96, pp. 45-64, 1939.

10. McMahon, T. A., *Muscles, Reflexes, and Locomotion,* Princeton University Press, Princeton, NJ, 1984.

11. McGinnis, P.M., *Biomechanics of Sport and Exercise*, Human Kinetics, Chamapaign, IL, 1999.

12. Harry J.D., A. W. Ward, N. C. Heglund, D. L. Morgan, and T. A. McMahon, "Cross-bridge cycling theories cannot explain high-speed lengthening behavior in frog muscle," *Biophys J,* Vol. 57, pp. 201–208, 1990.

13. CYBEX NORM System User's Brochure, CYBEX International, NY, 1997.

14. Peskin, C. S., *Programs for Modelling and Simulation in Medicine and the Life Sciences*, *2nd ed*., New York: Springer-Verlag, 2002. Available: http://www.math.nyu.edu/faculty/peskin

15. Marieb, E. N., *Human Anatomy and Physiology,* Benjamin-Cummings, Redwood City, Calif., 1995.

16. Fuglevand, A. J., "Resultant muscle torque, angular velocity, and joint angle relationships and activation patterns in maximal knee extension," In: *Biomechanics X-A,* edited by B. Jonsson, Champaign, IL: Human Kinetics, 1987, pp. 559–565.

17. Wickiewicz, T. L., R. R. Roy, P. L. Powell, J. J. Perrine, and V. R. Edgerton, "Muscle architecture and force-velocity relationships in humans," *J Appl Physiol,* Vol. 57, pp. 435–443, 1984.

18. Lieb, F. J., and J. Perry, "Quadriceps function: an anatomical and mechanical study using amputated limbs," *J Bone Joint Surg Am,* Vol. 50, pp. 1535–1548, 1968.

19. Bobbert, M. F., and G. J. Van Ingen Schenau, "Isokinetic plantar flexion: experimental results and model calculations," *J Biomech,* Vol. 23, pp. 105–119, 1990.

20. Thorstensson, A., G. Grimby, and J. Karlsson, "Force–velocity relations and fibre composition in human knee extensor muscles," *J Appl Physiol*, Vol. 40, pp. 12–16, 1976.

21. Spoor, C. W., and J. L. Van Leeuwen, "Knee muscle moment arms from MRI and from tendon travel," *J Biomech,* Vol. 25, pp. 201–206, 1992.

22. Perrine, J. J., and V. R. Edgerton, "Muscle force-velocity and power-velocity relationships under isokinetic loading," *Med Sc .Sports Exerc,* Vol. 10, pp. 159–166, 1978.

23. Wickiewicz, T. L., R. R. Roy, P. L. Powell, J. J. Perrine, and V. R. Edgerton, "Muscle architecture and force-velocity relationships in humans," *J Appl Physiol,* Vol. 57, pp. 435–443, 1984.

24. Kawakami, Y., K. Kubo, H. Kanehisa, and T. Fukunaga, "Effect of series elasticity on isokinetic torque-angle relationship in humans," *Eur J Appl Physiol,* Vol. 87, pp. 381-387, 2002.

25. Ichinose, Y., Y. Kawakami, M. Ito, H. Kanehisa, and T. Fukunaga, "In vivo estimation of contraction velocity of human vastus lateralis muscle during 'isokinetic' action," *J Appl Physiol,* Vol. 88, pp. 851-856, 2000.

26. Reeves, N. D. and M. V. Narici, "Behavior of human muscle fascicles during shortening and lengthening contractions in vivo," *J Appl Physiol ,* Vol. 95, pp. 1090-1096, 2003.

27. Kawakami, Y., T. Muraoka, S. Ito, H. Kanehisa, and T. Fukunaga, "In vivo muscle fibre behavior during counter-movement exercise in humans reveals a significant role for tendon elasticity," *J Physiol,* Vol. 540, pp. 635–646, 2002.